

# An analytical approach to the estimation of vehicular communication reliability for intersection control applications

Tibor Petrov<sup>a,\*</sup>, Ilya Finkelberg<sup>d</sup>, Peter Počta<sup>b</sup>, Ľuboš Buzna<sup>a,c</sup>, Nina Zarkhin<sup>d</sup>, Ayelet Gal-Tzur<sup>d</sup>, Tomer Toledo<sup>d</sup>

<sup>a</sup> Department of International Research Projects—ERAdiate+, University of Žilina, Žilina, Slovakia

<sup>b</sup> Faculty of Electrical Engineering and Information Technology, University of Žilina, Žilina, Slovakia

<sup>c</sup> Faculty of Management Science and Informatics, University of Žilina, Žilina, Slovakia

<sup>d</sup> Transportation Research Institute, Technion—Israel Institute of Technology, Haifa, Israel

## ARTICLE INFO

### Keywords:

Connected and automated vehicles  
Communication failures  
Vehicular communication reliability estimation  
Road intersection control  
Emergency vehicle preemption

## ABSTRACT

Connected and automated vehicles bring the capability to generate traffic data for intersection control applications. Unfortunately, for various reasons, such as signal blocking and interference, vehicles may experience communication failures leading to inefficiencies, e.g., unnecessarily long waiting queues, increased noise and greenhouse gas emissions or increased delays of emergency vehicles at intersections resulting in lower life-saving rates. This paper proposes an analytical approach to estimate vehicular communication reliability for road intersection control applications. The road segment in front of the intersection is divided dynamically into two areas. Due to the physical proximity to the roadside unit, the adjacent area is assumed to have more reliable communication than the more distant area. Consequently, the information about the approaching traffic in the more distant area is deduced from received communication in both areas. The effectiveness of the proposed method is verified by simulation experiments. First, we evaluate the communication reliability estimator by prediction accuracy metrics. Second, we study the benefits of the deployment of this estimator for emergency vehicle preemption. Our results provide evidence that the estimator has the potential to improve the performance of intersection control applications.

## 1. Introduction

A near-future introduction of the connected vehicle (CV) technology is expected to improve traffic and vehicle control through driving assistance, collision avoidance and extended traffic management applications [1]. CV telematics data can be utilized to enhance the efficiency of traffic management and control, most notably intersection signal control, by identifying in advance and constantly tracking the exact positions of approaching vehicles, getting more accurate traffic status measurements and developing more efficient prioritization schemes.

Even without considering hardware failures and communication system overload, the baseline performance of vehicular communication systems is not perfect. The urban setting, where vehicular communication often takes place, is a very challenging environment for any mobile wireless communication system. Narrow streets, high-rise buildings and many other static and dynamic objects result in severe obstacle shadowing, multipath signal propagation and fading. Furthermore, the

operation of many other communication systems in the same area contributes to increased interference. All those factors may contribute to the suboptimal performance of vehicular communication systems [2,3].

Communication failures may negatively affect the efficiency of services that utilize the data generated by CV technologies. A prominent example is an emergency vehicle (EV) preemption system. Most emergencies in urban areas require the presence of an emergency response crew on site. Emergency vehicles need to reach the site as quickly and safely as possible to minimize damage to life and property, where even a slight delay can lead to a significant increase in cost and chances of loss of life [4,5]. As the population continues to grow rapidly, so does road congestion in the city centers, which increases emergency vehicles' response times. Signalized intersections are obvious obstacles that delay emergency vehicles. To facilitate a smoother intersection crossing, a preemption module can be implemented to identify the traffic situation at the intersection and provide an approaching EV with the appropriate right-of-way time window so the EV will experience zero or minimal de-

\* Corresponding author.

E-mail address: [tibor.petrov@uniza.sk](mailto:tibor.petrov@uniza.sk) (T. Petrov).

lay. A study presented in [6] attributes a potential increase of between 32% and 90% in cumulative survival ratio (CSR) gains for acute and critically ill patients to the implementation of preemption at signalized intersections. These benefits could be negatively affected by communication failures.

## 2. Literature review

In this section, we provide an overview of the available literature dealing with the reliability of the vehicular communication technologies and its estimation. Furthermore, we analyze the relevant literature aimed at the application of the CV technology to prioritize emergency vehicles (EVs) in an urban traffic setting, as we assume this is one of the areas where implications of erroneous communication may cause the most serious societal consequences.

### 2.1. Communication failures in CV technologies

Message loss in a wireless communication system is caused by system overload, hardware failure, insufficient signal strength at the receiver caused by signal attenuation and fading, naturally- or artificially-induced interference and high levels of noise in the communication chain. Even without considering hardware-related communication failures, the communication performance of Dedicated Short-Range Communications (DSRC) as well as Cellular Vehicle-to-Everything (C-V2X) can often be limited by environmental factors. For example, Lee et al. [7] conducted a comparative experimental study measuring the performance of DSRC and Wi-Fi in different locations and under varying weather conditions. The authors conclude that compared to laboratory measurements, the outdoor performance of DSRC in terms of packet loss and jitter deteriorated considerably, especially at longer communication distances, i.e., above 180 meters. The DSRC performance degraded even further in rainy weather. Bai et al. [8] performed measurements at an urban/suburban freeway to analyze the application-level reliability of DSRC communication for vehicle safety applications. They found that the Packet Delivery Ratio (PDR) drops quickly with increased distance between the communicating nodes. While the measured PDR is around 90% at 100 meters, it drops to values as low as 67% and 58% at 300 and 400 meters, respectively. Very similar figures are reported also by [9]. The authors evaluated the Vehicle-to-Vehicle (V2V) communication reliability based on experimental data, collected at an urban expressway. The data show that even in Line-of-Sight (LOS) communication scenarios, PDR drops significantly for communication distances greater than 150 meters. The reported LOS PDR is below 70% at 200 meters and 67% at 300 meters. The performance in Non-Line-of-Sight (NLOS) communication scenarios is even worse. PDR at 200 and 300 meters in this case reaches only 65% and 42%, respectively. Gonzalez et al. [10] executed a performance comparison of the mode 3 and mode 4 of the 4G-based C-V2X for the V2V communication in terms of the packet delivery ratio. They showed that the centralized mode, i.e., the mode 3, obtained the higher PDR levels for the larger coverage distances than the non-centralized one, which does not demand cellular network coverage and vehicles can control the usage of radio resources by deploying the pre-established mechanism. Moreover, they also found, similarly as in the DSRC case (see the text above for more details), that the PDR drops quickly with increased distance between the communicating nodes in the case of the both modes. While the PDR for the packet transmission rate of 50 packets per second is around 97% and 75% at 100 meters, it drops to 15% and 38% at 400 meters for the mode 3 and mode 4 respectively. Ghodhbane et al. [11] studied the performance of the mode 4 of the 4G-based C-V2X considering event-based Decentralized Environmental Notification Messages as well as Cooperative Awareness Messages (CAM) and the V2V communication. The results show that a performance of 4G-based C-V2X is significantly affected by traffic load and sensing-based semi persistent

scheduling mechanism parameters, i.e., sensing window and keep probability. Moreover, when it comes to the PDR behavior, they report a rather similar trend for a highway scenario as the one reported in [10] but naturally with a bit more positive PDR levels. Regarding the DSRC and 4G-based C-V2X performance benchmark, the interested reader is referred to the following studies [12–24]. Moreover, when it comes to the 4G-based and 5G-based C-V2X performance benchmark, the interested reader is referred to [25].

With such a high level of packet loss reported above for both communication technologies, i.e., DSRC and C-V2X, many services relying on real-time data transmitted via Vehicle to Everything (V2X) communication might be severely impacted. Liu et al. [26] demonstrated how a failure in communication of a single vehicle destabilizes a CV platoon. Furthermore, the authors developed a CV following model which compensates for disruptions in communication topology and perception inaccuracies to stabilize platoons. Therefore, it is important to be able to estimate the instantaneous message loss ratio in the selected part of the communication network, so that mechanisms to compensate for the lost vehicular data might be deployed.

Traditional methods for estimation of the message loss ratio in wireless networks are based mostly on the transmission of probe messages. In the case of Vehicular Ad hoc Networks (VANETs), this approach has two major limitations. Firstly, the periodic transmission of probe messages presents a significant overhead in bandwidth-limited VANETs. Secondly, the size of a probe message is usually much smaller than the size of a message carrying payload data, hence it is much less prone to bit-error-induced losses than the typical payload messages. To limit the network overhead induced by frequent transmissions of probe messages, Jiang et al. [27] proposed an estimation algorithm for packet loss on VANET which is based on the general statistical properties of packet loss rate over distance in VANET. The algorithm uses the Gaussian Mixture Model (GMM) and a limited number of probe packets to estimate the packet loss ratio probability density. The proposed algorithm is more bandwidth-efficient compared to the traditional methods for packet loss estimation in wireless networks, however, it assumes the statistical model of packet loss in VANET to be known. This can result in a rather high estimation error in the case when the communication environment does not match the statistical model. Alzamzami and Mahgoub [28] proposed an enhanced directional greedy forwarding scheme that incorporates a link quality estimation. The link quality estimation is based on the broadcasting of HELLO messages to consider the loss rate in both communication directions. For that sake, the HELLO messages need to be acknowledged, which further increases the signalization overhead.

To sum up, to the best of our knowledge, published approaches so far involve the probing technique, which generates additional traffic load. So, it is rather ineffective in the context of bandwidth-limited communication environments, e.g. VANET, etc. This fact has motivated us to develop a new approach mitigating this limitation. Furthermore, as demonstrated in our previous work [29], communication failures may significantly decrease the efficiency of intersection control algorithms. In that paper, we tested a simple mechanism to estimate the number of vehicles approaching an intersection that compensates for communication failures. This solution helps to decrease the effects of communication failures on intersection control algorithms, but it is application-specific. In this paper, we propose and evaluate an application-agnostic approach to estimate communication reliability in the neighborhood of a road intersection.

### 2.2. Approaches to EV prioritization in CV environment

Application of vehicular communication performance estimation can bring the highest benefits at intersections. Here, the probability of gathering a large number of communicating vehicles in a short time and a limited area is the highest. Increased density of communicating nodes may severely affect the performance of the traffic control

by overloading the communication channel [30]. Inefficient traffic control leads not only to economic and environmental damage caused by congestion, such as increased fuel consumption, air pollution, time loss and is a source of annoyance for drivers and passengers, but it may turn deadly in situations requiring the quick intervention of emergency response services [31]. Therefore, communication performance estimation together with missing data compensation mechanisms is of utmost importance for applications such as intersection preemption for emergency vehicles in a CV environment.

There are several ways to use CV technology to facilitate emergency vehicle traversal along signalized urban arterials. Su et al. [32] developed a dynamic queue-jump method, where an EV sends instructions via V2V interface to the downstream vehicles to make them clear its lane. In reality, this approach might be less efficient in dense urban centers where clearing the lane might be impossible due to limited space. Xie et al. [33] suggested that in addition to broadcasting a V2V warning message to drivers in the corresponding area, a signal preemption is activated once the emergency vehicle is within a fixed distance from the intersection. In this scheme, providing the right-of-way to the EV is made as soon as possible and the green light is extended as much as necessary, i.e., until the EV crosses the intersection. However, such an approach might lead to extensive delays of the conflicting movements at the intersection.

While [33] and [34] focused on minimization of EV delay as the top priority guiding the signal control logic, the effects on non-priority vehicles need to be considered and reduced if possible. One way to achieve this is to minimize the required green duration for EV preemption by estimating the moment in time when an EV Signal Group (SG) needs to be switched to green. Qin and Khan [35] proposed a preemption model where a minimum notification period is calculated, i.e., the point when the preemption green needs to be activated, represents a sum of switchover to green time, queue discharge time and safety time interval which ensures large enough gap between the last vehicle in the queue and the incoming EV for safety reasons. Paruchuri [36] proposed a similar approach to minimize the disruption to normal traffic by adaptively adjusting the preemption duration based on the existing traffic conditions, i.e., constantly calculating the time required to switch to green and to clear the queue. In [35], once the EV crossed the stop line, a recovery period is activated, where green duration for conflicting movements is optimized to shorten the queues to their predefined acceptable lengths.

One of the main inputs to the preemption control algorithm is the EV's estimated time of arrival (ETA). It directly influences the control decisions required to eliminate or minimize delay to an approaching vehicle while keeping the duration of disturbance to conflicting movements minimal. A comprehensive review of preemption methods [37] states that there is a gap between a calculated ETA and the actual arrival time as theoretical models are based on calculations that do not necessarily account for all the factors that impact the EV's movement. In the case of CV, this gap might be even larger, as the majority of models are based on the unrealistic assumption of perfect communication. Imperfect communications are rarely considered in traffic control schemes in a connected vehicle environment. In a recent review of Traffic Control strategies for Emergency Vehicles [38] the issue of reducing interference and communication costs is described as one of the future research directions. Despite this fact, the most recent research on Emergency Vehicles preemption in Connected Vehicles environment [39,40] still follows the common practice of not taking into account the effects of imperfect communications. Perfect communication assumptions may lead to inefficient performance and increased delays in scenarios, where communication disruptions are present. Our work addresses this gap in two ways:

1. Considering communication failures and the properties of traffic flows, an analytical Message Loss Ratio estimator is developed and its accuracy is evaluated by prediction accuracy measures.

2. An utilization of the suggested approach is showcased in a traffic signal control algorithm with EV prioritization. By utilizing the knowledge of the estimated magnitude of imperfect communication conditions, an EV estimated ETA is adjusted to compensate for uncertainties in the assessment of the traffic situation. Using simulation tools, we show that such an adjustment reduces delays of EVs at intersections. The reduction may be critical to avoid a possible increase in injury severity, loss of life and property damage.

The paper is organized as follows: the next section presents the MLR estimator and the modeling framework. Section 4 introduces MLR estimator performance evaluation using prediction accuracy metrics. Section 5 is showcasing the application of the MLR estimator to the emergency vehicle preemption. Finally, the discussion and conclusions are presented in Section 6.

### 3. Materials and methods

The section provides background information. The concept of the MLR estimator, together with necessary justifications, is presented in Section 3.1. Section 3.2 introduces the integrated traffic and communications modeling framework.

#### 3.1. MLR estimator

The status of communication networks can be quantified by the Message Loss Ratio (MLR):

$$MLR = \begin{cases} 1 - \frac{N_{rcvd}}{N_{snt}}, & \text{if } N_{snt} > 0 \\ 0, & \text{otherwise} \end{cases}, \quad (1)$$

where  $N_{rcvd}$  and  $N_{snt}$  are the true numbers of received and sent messages, respectively. In an environment with faulty communication, the MLR value needs to be estimated. Nowadays, problems in estimating a quantity from data are often handled by statistical or machine-learning approaches [41]. This requires the availability of data for the training of models and predictions, i.e., historical records of MLR values and features that contain a signal correlated with MLR values. Typically, there is no MLR data for road network intersections. Therefore, here we propose an analytical approach, where the estimation of the MLR value is derived from communication and traffic data that can be easily collected and processed. The used notation is summarized in Table 1.

The proposed concept is based on the assumption that communication reliability mainly depends on the distance between the sender and receiver as illustrated in Fig. 1. When the distance is short, communication is expected to be more reliable as it is happening in a communication range of vehicles. To model this assumption, the length of the observed area  $P$  in front of the intersection can be split into a part with mostly reliable communication  $C$  and a part with mostly unreliable communication  $U$ . Hence, the length of the area  $C$  is equal to the average effective communication range of vehicles. By the effective communication range, we mean a dynamic range reflecting the current transmission conditions. Thus, the communication range can vary depending on the density of traffic. As the reliability of the communication strongly affects an ability to infer the number of lost messages  $N_{lost}$  from the number of vehicles approaching the intersection, we apply different approaches to the area within the communication range and to the area outside of the communication range. Within the communication range, the number of lost messages  $N_{lost}^C$  can be estimated by keeping track of the vehicles that have communicated previously and are still likely to be approaching the intersection. Important prerequisites for this task are knowledge of the vehicles' message generation frequency and positions. A Road Side Unit (RSU) can extract the sender's position from the Cooperative Awareness Messages (CAMs), which are broadcasted periodically by each connected vehicle. The message generation frequency depends on the specific Cooperative

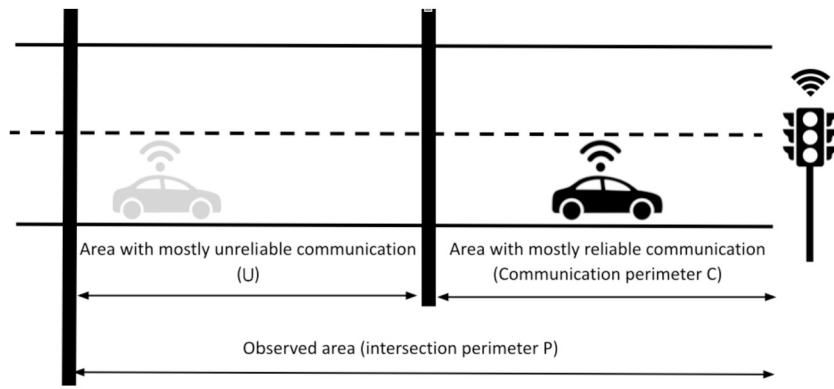


Fig. 1. Schematic illustrating the modeling approach considering the dependence of the communication reliability on the distance from the intersection.

**Table 1**  
Table of used symbols in the description of the MLR estimator.

Symbol	Description
$P$	The observed area in front of the intersection.
$C$	The part of the area adjacent to the intersection with mostly reliable communication.
$U$	The part of the area in front of the intersection with unreliable communication.
$L_{CV}$	The list of communicating vehicles that according to their last position have not yet crossed the intersection. The roadside unit maintains the list.
$N_{CV}$	The number of vehicles in the list $L_{CV}$ .
$L_{AV}$	The list of vehicles that successfully sent a message to the roadside unit within the last $t_2$ time units. The roadside unit maintains the list.
$N_{rcvd}$	The number of received messages by the roadside unit within an observed time window.
$N_{snt}$	The number of sent messages to the roadside unit within an observed time window.
$N_{lost}$	The number of lost messages given by the difference between $N_{snt}$ and $N_{rcvd}$ .
$N_{lost}^C$	The estimated number of lost messages within the area $C$ and period $t_2$ . It is derived from previously received communication.
$N_{lost}^U$	The estimated number of lost messages within the area $U$ and period $t_2$ . It is derived from the flow intensity estimate.
$F$	The estimated intensity of the vehicular flow.
$t_1$	The length of the period given by the periodicity of sending communication messages. In experiments, the value of 1 s was used.
$t_2$	The length of the period selected for estimation of quantities. In experiments, the value of 600 s was used.
$t_U$	The average time the vehicles spend in the area $U$ .

Intelligent Transport System (C-ITS) application and is either known or can be easily estimated from the received data. It is assumed that this frequency does not vary in time, which is currently the case in the context of the Cooperative Awareness basic service [42]. It is worth noting here that a suitable CAM message generation frequency depends on a position and velocity of vehicles. The value of the frequency can be specified by the TGen parameter.

The RSU maintains a list of communicating vehicles (denoted as  $L_{CV}$ ), i.e., vehicles that have successfully delivered a message and according to their last known position have not yet crossed the intersection. A vehicle is detected to have left the intersection by receiving a CAM message with the vehicle position indicating the change from an incoming to an outgoing lane. The RSU is usually installed very close to the intersection, therefore, it is reasonable to assume that at least one message indicating the vehicle has crossed the intersection will be received and the vehicle is removed from the  $L_{CV}$ . For each time window  $t_1$ , which equals to the vehicles' message generation period, we estimate the number of lost messages  $N_{lost}^C$  as a difference between the number of vehicles in the list  $L_{CV}$  ( $N_{CV}$ ) and the number of the successfully received messages  $N_{rcvd}$  within the time window. To estimate the number of lost messages  $N_{lost}^U$  in the area out of the communication range, we define a time window of duration  $t_2 > t_1$

(see Fig. 2a) and estimate the average intensity of vehicles  $F$  arriving into the area  $U$ . Assuming that the intensity of vehicles arriving into  $U$  is the same as for the area  $C$ , we estimate the value  $N_{lost}^U$  in two steps:

- 1. Estimation of the average time,  $t^U$ , a vehicle spends in the area  $U$ :** When a vehicle enters the area  $P$  it records the current time. This time information is included in every future message sent by the vehicle. When RSU receives the first message from a vehicle, it calculates  $t^U$  as the difference between the current time and the time found in the message and the vehicle ID is stored in the list of all vehicles  $L_{AV}$ .
- 2. Estimation of the average intensity,  $F$ , of the arrival flow of vehicles to the area  $C$ :** At the end of every time window  $t_2$ , the value  $F$  is updated by dividing the length of the list  $L_{AV}$  by  $t_2$  and the list  $L_{AV}$  is emptied.

Values  $F$  and  $t^U$  are then used to estimate the average number of the lost messages in the area  $U$  as follows:

$$N_{lost}^U = t^U F. \quad (2)$$

An overall  $\overline{MLR}$  value is estimated at the end of every time window  $t_1$  (see Fig. 2c) by using the following formula:

$$\overline{MLR} = \begin{cases} 1 - \frac{N_{rcvd}}{N_{rcvd} + N_{lost}^C + N_{lost}^U}, & \text{if } N_{rcvd} + N_{lost}^C + N_{lost}^U > 0 \\ 0, & \text{otherwise} \end{cases}. \quad (3)$$

The implementation of the proposed MLR estimation approach is available for the scientific community on GitHub [43].

### 3.2. Simulation framework

The simulation framework used to assess the performance of MLR estimation and its showcasing to the EV preemption is based on the work published in [44]. It employs the principles of the federated telco-traffic simulation [45–47] and consists of Objective Modular Network Testbed in C++ (OMNeT++) [48] as a communication network simulator, PTV VISSIM as a traffic simulator, MLR estimator module and an interface facilitating bi-directional, real-time data exchange between the components. As an alternative to PTV VISSIM, another state-of-the-art traffic simulator (e.g. SUMO [49]) could be used. To simulate communication protocols specific to connected vehicles, Veins [46], Simu5G [50] and INET [51] simulation frameworks for OMNeT++ were used. The simulation workflow is depicted in Fig. 3. The simulation time is split into equal time periods of length  $\Delta t$ . After the launch of the simulation, VISSIM simulates the first  $\Delta t$  period, stores the attributes of communication module-equipped vehicles in a shared file and waits for the outputs from OMNeT++ and MLR estimator. The vehicle attributes include ID, geo-

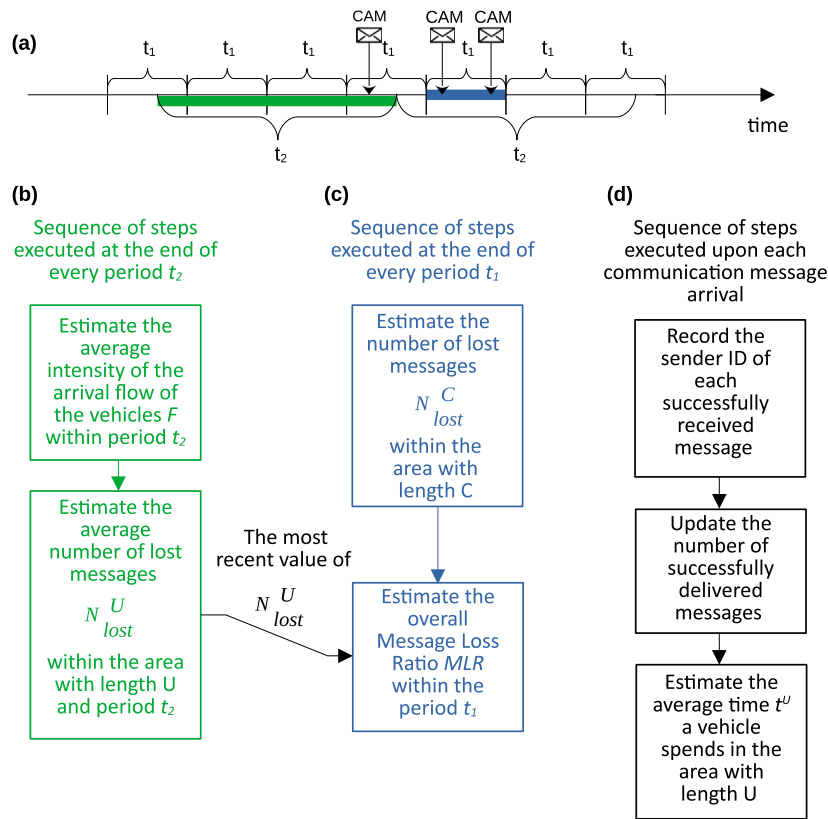


Fig. 2. Updates of MLR estimates on two different time scales  $t_1$  and  $t_2$ . (a) Overlays of periods  $t_1$  and  $t_2$  and illustration of communication messages arrivals to RSU. (b) The sequence of steps executed at the end of every period  $t_2$ ; (c) The sequence of steps executed at the end of every period  $t_1$ . (d) The sequence of steps executed upon each communication message arrival.

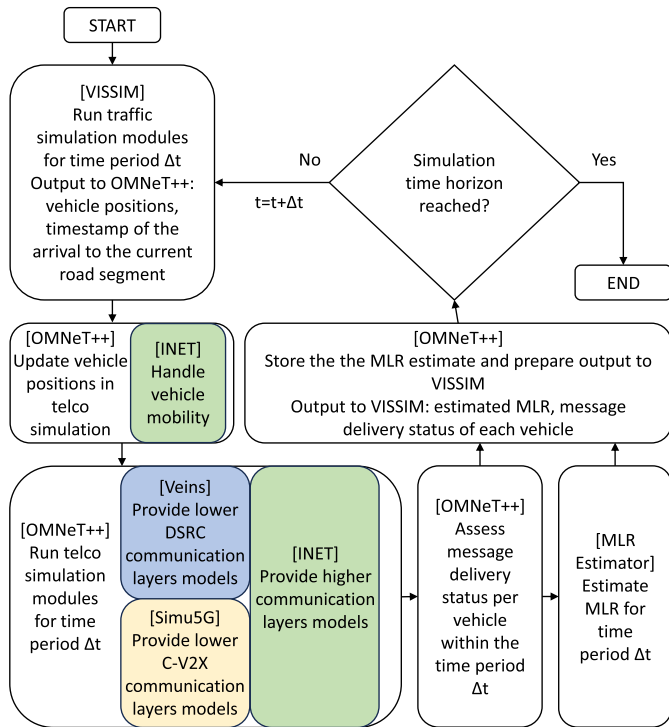


Fig. 3. The simulation workflow diagram.

graphic location, speed, lane index and timestamp of the arrival to the current road segment for each vehicle. This information is utilized by OMNeT++ to update the positions of vehicles in the telco simulation

and to compute the per-vehicle message delivery status, whether a communication message from the corresponding vehicle has been delivered to the RSU within the corresponding  $\Delta t$  period in the telecommunication domain. The information from successfully received messages is fed into the MLR estimator module, which uses it as input for the MLR estimation algorithm described in Section 3.1. MLR estimator outputs the estimated MLR value to a shared folder. At the end of the corresponding  $\Delta t$  period, OMNeT++ and MLR estimator are suspended until updated vehicle attributes are provided by VISSIM for the next  $\Delta t$  period. The message delivery status and estimated MLR value are loaded by VISSIM, which updates the traffic simulation modules accordingly and the simulation cycle repeats until the simulation time horizon is reached.

#### 4. MLR estimator performance evaluation

In this section, we evaluate the performance of the MLR estimator by prediction accuracy metrics. We start by introducing the simulation settings and next we describe the results of numerical experiments.

##### 4.1. Methodology

The simulated area and the detail of the intersection are depicted in Fig. 4. The traffic model is based on a real intersection of Hanita-Trumpeldor streets in the city of Haifa, Israel. For the purpose of this work, a CV control scheme is utilized. The detailed description of the CV control scheme algorithm can be found in [29]. The investigated intersection model was equipped with a roadside unit (RSU) connected to the intersection controller (IC) using a wired lossless communication link introducing negligible communication delay. The roadside unit receives communication messages including vehicle telemetry data and passes them to the IC.

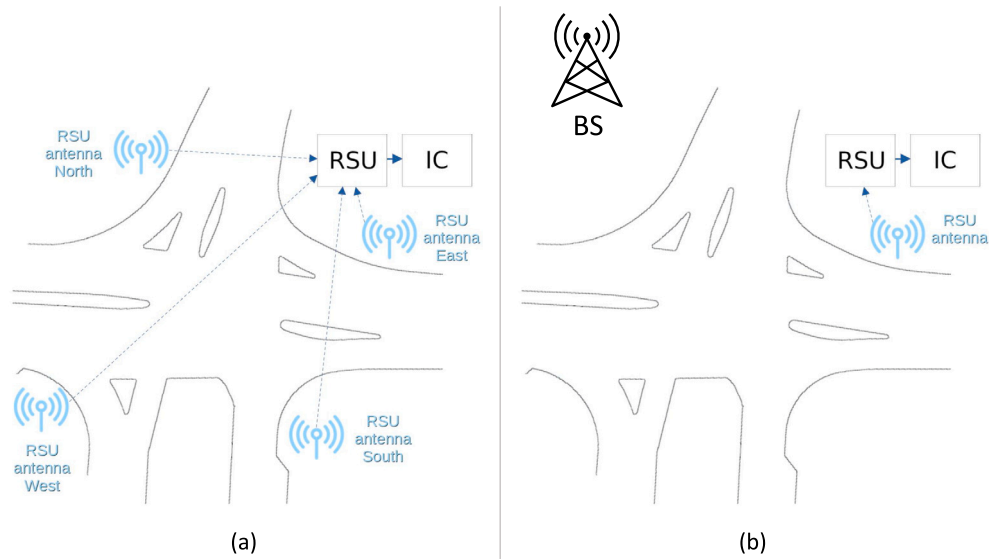


**Fig. 4.** Detail of the controlled intersection for (a) DSRC simulation scenario and (b) 4G-based C-V2X and 5G-based C-V2X simulation scenario. RSU block represents the Roadside Unit and the IC and BS blocks represent the Intersection Controller and the Base Station respectively.

**Table 2**

Dedicated Short-Range Communications (DSRC) communication network simulation parameters and their values.

Parameter	Value	Parameter	Value
Access Layer specification	ETSI ITS-G5 - Based on IEEE 802.11 OCB (historically referred to as 802.11p), [52]	Ground type	Flat asphalt roadway
Message service	CAM-like - Periodic, fixed-length unicast messages (from vehicles to RSU), [53]	Permittivity of asphalt at microwave frequencies	4.75, [54]
Message length	300 B - Assuming transmission of basic Cooperative Awareness Service data and a security header, [55]	Vehicle antenna height	1.895 m, [46]
Carrier frequency	5,900 MHz - Corresponding to ETSI ITS-G5 Control Channel, [56]	RSU antenna height	5.897 m, [29]
Channel bandwidth	10 MHz - Corresponding to ETSI ITS-G5 Control Channel, [56]	Antenna type	Isotropic antenna
Data rate	6 Mbps - Corresponding to ETSI ITS-G5 default data rate, [56]	Background Noise (parameter background Noise in Veins)	-86 dBm
Transmitter power	20 mW	SNR Penalty in East approach	0 dB, 20 dB, 25 dB, 30 dB
Background noise power	-86 dBm - Severe noise conditions	Default SNR Penalty	0 dB
Path loss model	Two Ray Interference, [46]		

We evaluated the performance of the MLR estimator using three different communication technologies, i.e., DSRC, 4G-based C-V2X and 5G Standalone (5G SA)-based C-V2X communication in Vehicle-to-Network (V2N) configuration. For evaluation of the MLR estimator performance in C-V2X environment, we selected communication through the infrastructural V2N mode using the standard Uu cellular interface instead of the sidelink PC5 interface for two reasons. First, it is expected that future digital infrastructure will utilize the cellular Uu interface for the long-range communication with vehicles due to its longer range compared to the range provided by the PC5 interface. Second, our aim is to evaluate the MLR estimator performance using a diverse set of the communication technologies. DSRC is based on the ad-hoc network paradigm. C-V2X with the Uu interface represents the centrally managed network paradigm. Thus, this way we evaluate the MLR estimator using two different network paradigms.

In the case of the DSRC, the RSU is equipped with four antennas, one per each major intersection leg to maximize the probability of Line of Sight (LOS) communication with vehicles, thus increasing the communication range, see Fig. 4a for more detail. In experiments using the C-V2X communication technologies, the RSU uses one antenna only to communicate through the Uu interface with a base station located in the close proximity of the intersection, see Fig. 4b for more detail. Each vehicle in the simulation transmits communication messages periodically to the RSU using one of the abovementioned communication

technologies. The communication link between vehicles and RSU might be subject to effects degrading the communication performance such as attenuation, noise, interference and fading. In the case of the DSRC technology, the attenuation is modeled by the Two Ray Interference path loss model [46], commonly used in vehicular network simulations. The effects of noise are modeled using the Veins framework's inbuilt background noise parameter. The attenuation of C-V2X channel is modeled using the 3D-Uma Path Loss Model as defined in 3GPP TR 36.873 [57] and implemented in the Simu5G framework. To quantify the combined effect of interference and fading, we introduce the Signal-to-Noise Ratio (SNR) Penalty parameter. It is worth noting here that the SNR Penalty parameter represents the impact of environmental conditions on the communication between vehicles and the RSU. SNR Penalty is implemented in the simulation model by varying the sensitivity of RSU receivers and describes the drop of SNR compared to the scenario with no interference and fading effects. A short list of the communications-related parameters is presented in Table 2 and 3. Significant differences exist between the access technologies of 4G-based and 5G-based C-V2X in terms of operation modes, Medium Access Layer, and Physical Layer. However, if possible, the same values of the communications-related parameters were applied for the 4G-based and 5G-based C-V2X in order to allow a fair comparison. Parameters, which are not explicitly mentioned in Tables 2 and 3, were set to their default values according to the documentation of the respective simulation frameworks [58,50]. The

**Table 3**

Cellular Vehicle-to-Everything (C-V2X) communication network simulation parameters and their values applied to both technologies, i.e., 4G-based C-V2X and 5G-based C-V2X.

Parameter	Value	Parameter	Value
Access Layer specification	Based on 3GPP release 16, [59]	Path loss model	Free Space Path Loss
Message service	CAM-like - Periodic, fixed-length unicast messages (from vehicles to RSU), [53]	Vehicle antenna height	1.895 m, [46]
Message length	300 B - Assuming transmission of basic Cooperative Awareness Service data and a security header, [55]	RSU antenna height	5.897 m, [29]
Carrier frequency	2,400 MHz	Antenna type	Isotropic antenna
Channel bandwidth	20 MHz	SNR Penalty in challenging communication scenario	20 dB
Base station transmitter power	40 W, [60]	Default SNR Penalty	0 dB
Vehicle transmitter power	400 mW, [50,60]		

extended list of the simulation parameters and their values is provided, for the convenience of the interested reader, in Tables A.9 and A.10 for the DSRC and C-V2X technologies, respectively. The communication network simulation files for the OMNeT++ including all the configurations are available for the scientific community on GitHub [43].

Three objectives guided the performance evaluation of the MLR estimator:

- to identify operational boundaries of the MLR estimator in terms of intersection leg length, traffic volume and Signal-to-Noise Ratio (SNR) Penalty,
- to examine the applicability of the proposed MLR estimator in terms of estimation accuracy,
- to showcase that the proposed MLR estimator is a communication technology agnostic.

The key performance indicator selected to quantify the performance of the estimator is the Mean Absolute Error:

$$MAE = \frac{1}{n} \sum_{i=1}^n |MLR_i - \overline{MLR}_i|, \quad (4)$$

where  $MLR_i$  is the  $i$ -th observation of the true value and  $\overline{MLR}_i$  is the corresponding estimated value. Furthermore, we considered the Spearman's Rank Correlation Coefficient:

$$\rho = 1 - \frac{6 \sum_{i=1}^n (R(MLR_i) - \overline{R(MLR)})^2}{n(n^2 - 1)}. \quad (5)$$

Both the true values of the Message Loss Ratio and their estimates are ranked over all  $i = 1, \dots, n$  observations, where  $R(\cdot)$  returns the rank.

To identify operational boundaries and examine the applicability of the MLR estimator we consider three simulation variables, i.e., intersection leg length (100 and 200 meters South approach length), traffic volume (200, 400, 600 and 800 vehicles per hour in South approach) and SNR Penalty (0, 20, 25 and 30 dB in East approach). It should be highlighted here that this was done only for the DSRC communication technology. We conducted five independent simulation runs for each combination of simulation variables. Since the estimation of the number of vehicles present in the area  $U$  contributes to the overall estimation of the MLR value, we first studied the impact of the length of the observed area and the vehicle volume on the estimation quality. The longer the length of the observed area, the more messages are unlikely to reach the RSU. Similarly, the increase in communication interference impacts communication performance by making the received signal harder to decode without errors by the receiver. Therefore, in the second performance evaluation scenario, we studied the impact of the SNR Penalty on the estimation quality. To vary the length of the observed area, we chose the South leg of the intersection, since it is the shortest leg of the Hanita/Trumpeldorf intersection. To study the impact of SNR Penalty on estimation performance we selected the East approach of the intersection since it is the approach with the highest traffic volume and therefore is expected to be affected by interference the most.

To showcase that the proposed MLR estimator is a communication technology agnostic we fixed the intersection leg length in the South approach to 100 m and traffic volume to 600 vehicles per hour and deployed the realistic range of the SNR Penalty, i.e. 0 and 20 dB. These values represent the result of the operational boundaries investigation. When it comes to the SNR Penalty, we limited the investigation to the boundary values, i.e. 0 dB and 20 dB, for the practical reasons. This investigation was naturally done for all the abovementioned communication technologies, i.e. DSRC, 4G-based C-V2X and 5G-based C-V2X communication. We conducted five independent simulation runs for each value of the SNR Penalty.

#### 4.2. Results

Tables 4 and 5 present the average values of performance indicators for each combination of the simulation variables. Values in bold identify the intersection leg, where the given simulation variable has been varied. For the remaining intersection legs, the simulation parameters were set to their default values, as described in Section 4.1. The average values of performance indicators indicate that the vehicle volumes play a crucial role in the accuracy of the estimation and increasing the intersection leg length slightly improves both the estimation accuracy and the correlation of the estimates. For both cases, i.e., 100 m leg length and 200 m leg length, the optimum performance of the MLR estimator is achieved for the vehicle volumes between 400 and 600 vehicles per hour (Table 4). Further increase in the number of vehicles does not bring any significant improvement. Furthermore, the estimation error is only marginally lower when the intersection leg length is doubled, suggesting that the quality of estimates is not strongly sensitive to the length of the observed area.

Figs. 5a-5d illustrate the quality of the estimation for four different values of traffic volume ranging from 200 to 800 vehicles per hour for a single simulation run. The figures clearly show that there is a positive correlation between the quality of estimation and traffic volume. This is caused by the variation in the number of communicating vehicles and hence the messages sent. The lower the number of messages, the larger the MLR value when a single message gets lost, as demonstrated by frequent MLR value spikes in Figs. 5a-5d.

In Table 5, we present the values of the Mean absolute error and Spearman's rank correlation coefficient obtained for four levels of SNR Penalty, i.e., 30 dB, 25 dB, 20 dB and 0 dB. It is worth reiterating here that the objective of this performance evaluation is to uncover the operational boundaries of the proposed MLR estimation approach. Therefore the values used herein were selected to represent both extremes of interference impact, i.e., extremely challenging communication environment and no interference impact. In both cases, the level of background noise is fixed at a very high value ( $-86$  dBm), so the communication environment is still challenging enough to observe increased MLR levels.

The results show a significant estimation error in the extremely challenging communication scenario, i.e., with the SNR Penalty value of 30 dB. With lowering the SNR Penalty to 25 dB, the Mean absolute error drops significantly and does not further improve with an additional decrease in the interference level. It is different for the Spearman's rank

**Table 4**

Average values of the Mean absolute error and Spearman's rank correlation coefficient of the estimated Message Loss Ratio (MLR) obtained for the DSRC technology and evaluated for different intersection approaches (South, East, North, West). In experiments, we fixed SNR Penalty to 0 dB and we varied vehicle volumes in the South approach considering values 200, 400, 600 and 800 vehicles per hour and the South approach length considering values 100 and 200 meters.

South approach length [m]	100				200			
	200	400	600	800	200	400	600	800
	Mean absolute error, MAE [%]							
South	12.71	5.08	3.89	3.18	13.69	4.86	3.06	2.95
East	7.12	9.79	8.33	10.24	7.73	8.08	10.43	8.98
North	3.47	3.48	2.66	4.97	3.49	3.87	2.56	3.87
West	6.78	7.54	6.82	7.27	6.91	8.15	7.51	7.26
	Spearman's rank correlation coefficient, $\rho$							
South	0.18	0.56	0.58	0.61	0.32	0.60	0.69	0.78
East	0.76	0.75	0.72	0.76	0.72	0.76	0.76	0.84
North	0.70	0.69	0.74	0.75	0.68	0.64	0.70	0.77
West	0.69	0.75	0.72	0.49	0.69	0.80	0.78	0.63

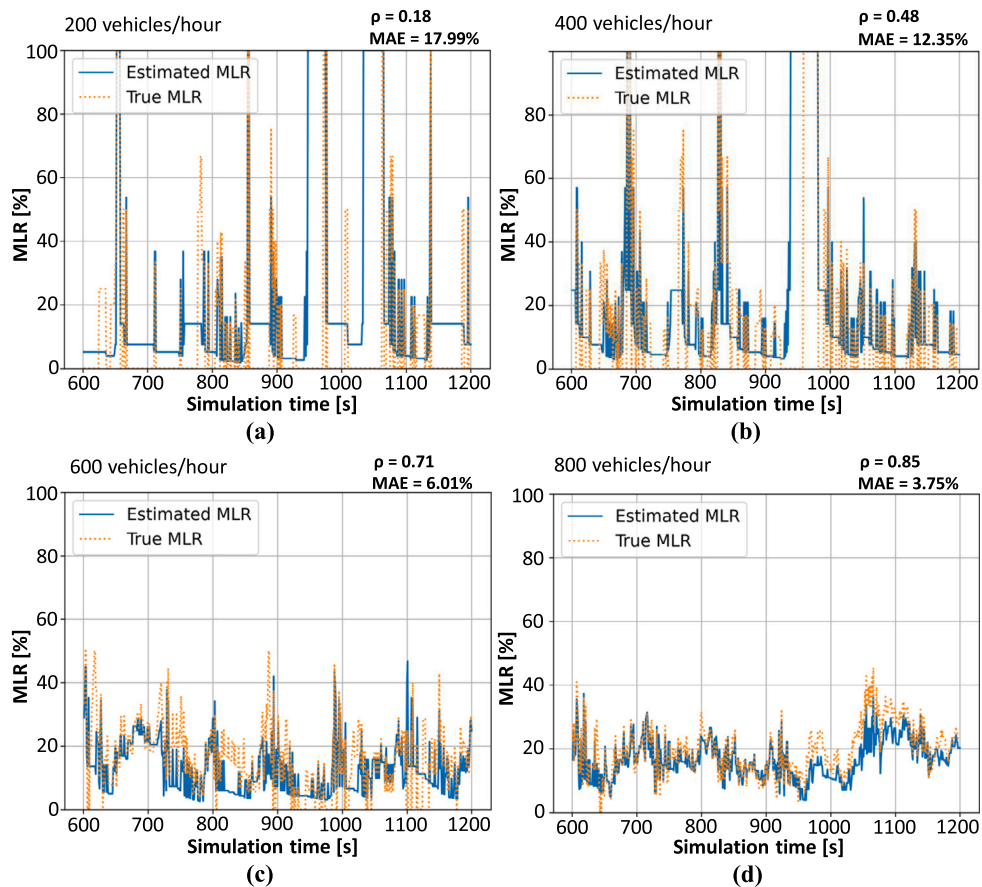


**Fig. 5.** The comparison of the true and estimated MLR values for a single typical simulation run obtained for the DSRC technology and the South approach, SNR Penalty = 0 dB, South approach length = 200 m and Traffic volume in (a) 200 vehicles/hour, in (b) 400 vehicles/hour, in (c) 600 vehicles/hour and in (d) 800 vehicles/hour.

correlation coefficient, whose value decreases in the scenario with no interference, i.e., with 0 dB SNR Penalty. The reason for the decrease in correlation might be a higher variance of the MLR over time in less challenging communication scenarios, which makes the estimation more difficult. As the true MLR when it comes to the SNR Penalty of 25 dB and 30 dB is well above 60% what is extremely high for practical deployments, we have decided to limit the range of the SNR Penalty from 0 dB to 20 dB for further investigations.

Some vehicles do not transmit successfully a single message to the RSU. The estimator is not aware of those vehicles and cannot use them

as input for MLR estimation. Such vehicles increase the estimation error. We refer to them as hidden vehicles. The problem with hidden vehicles cannot be mitigated without additional data collection measures. In this study, we considered information about hidden vehicles as inaccessible.

In Table 6 we benchmark the investigated communication technologies, i.e. the DSRC, 4G-based C-V2X and 5G-based C-V2X, for the different SNR Penalty values in terms of the average value of Mean absolute error (MAE). It should be noted here that the Spearman's rank correlation coefficient is not a suitable measure to compare the true and estimated MLR values in the context of the C-V2X technologies due to

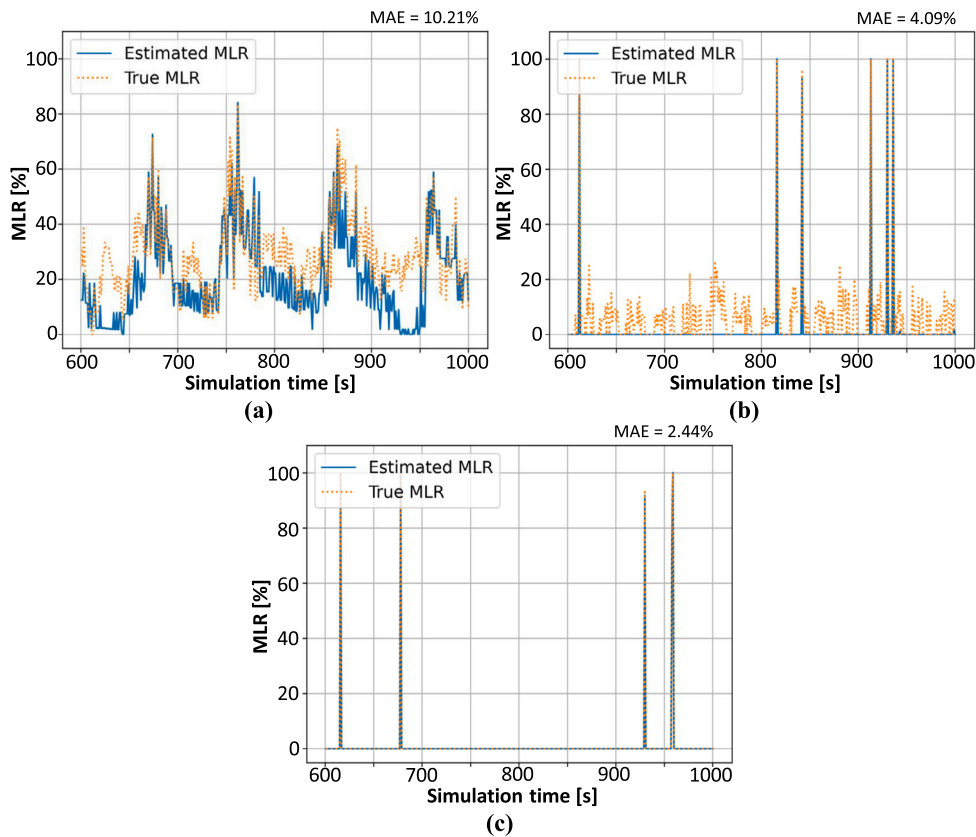


**Fig. 6.** The comparison of the true and estimated MLR values for a single typical simulation run obtained for the East approach, SNR Penalty = 0 dB and (a) DSRC, (b) 4G-based C-V2X and (c) 5G-based C-V2X.

**Table 5**

Average values of Mean absolute error and Spearman's rank correlation coefficient of estimated MLR evaluated for different intersection approaches (East, North, South, West) obtained for the DSRC technology. In experiments, we varied the SNR Penalty only in the East approach considering values 30, 25, 20 and 0 dB.

SNR Penalty [dB]	30	25	20	0
	Mean absolute error, MAE [%]			
East	<b>17.63</b>	<b>11.14</b>	<b>11.64</b>	<b>11.14</b>
North	3.46	3.01	4.38	2.66
South	4.25	3.74	3.81	3.89
West	6.3	6.81	6.74	6.82
	Spearman's rank correlation coefficient, $\rho$			
East	<b>0.82</b>	<b>0.86</b>	<b>0.81</b>	<b>0.69</b>
North	0.65	0.71	0.76	0.74
South	0.59	0.64	0.55	0.58
West	0.68	0.62	0.69	0.72

the strongly bimodal distribution of the MLR values, see Figs. 6b and 6c for more details. The true MLR values are most of the time close to zero and occasionally spike to the values being close to 100%, representing a rather challenging scenario for the MLR estimator. Thus, even small estimation errors can lead to a large difference in the rank. Therefore, we do not report the Spearman's rank correlation coefficient in Table 6. We can clearly see in Table 6 that all three technologies experience more or less the same trend, besides the 5G-based C-V2X for the SNR Penalty of 0 dB where the MAE is kept approximately at the same level. It is interesting to note here that the 4G-based C-V2X experiences a higher MAE than the remaining technologies. It seems to be caused by the less efficient resource scheduling algorithm deployed by the 4G-based C-V2X than that of the 5G-based C-V2X (see [25] for more details), inducing

the much higher and varying MLR than in the 5G case (see Figs. 6b and 6c for more details). Anyhow, the MLR estimator is still applicable in the context of the 4G-based C-V2X.

Figs. 6a-6c illustrate the quality of the estimation for a single typical simulation run for the investigated communication technologies. The figures clearly show that there is a similarity between the true and estimated MLR values. It can be clearly seen from the figures that the DSRC is the most challenging communication technology in terms of the MLR variation. On the basis of the results presented in Table 6 and Figs. 6a-6c, we can say that the proposed MLR estimator is the communication technology agnostic.

To the best of our knowledge there is no similar approach published in the literature, which we can benchmark the proposed approach with. Moreover, when it comes to the approaches based on the probing technique, mentioned in Section 2.1, which are anyhow conceptually different in terms of the design as well as the working principle, no implementation is unfortunately available, and their performance evaluations were done in different contexts. So, it is unfortunately not possible to benchmark a performance of the approach proposed in this work with those based on the probing technique. Anyhow, it should be stressed out here that we benchmark the proposed approach by deploying the ground truth values experienced in the context of our scenario/work. This represents, a natural way to evaluate the accuracy and reliability of the proposed approach.

## 5. EV preemption showcase

In this section, a showcase of possible MLR estimator utilization and its potential benefits are presented. The MLR estimator is used as an input in EV preemption signal control logic to provide a more robust preemption for an EV in cases of poor communications conditions,

**Table 6**  
Benchmark of the average values of Mean absolute error of the estimated MLR obtained for the DSRC, 4G-based and 5G-based C-V2X.

SNR Penalty [dB]	0			20		
	DSRC	4G C-V2X	5G C-V2X	DSRC	4G C-V2X	5G C-V2X
	Mean absolute error, MAE [%]					
East	11.14	6.02	0.44	11.64	18.44	6.53
North	2.66	1.06	1.03	4.38	5.67	0.68
South	3.89	0.41	0.75	3.81	11.99	0.48
West	6.82	4.53	0.28	6.74	15.38	4.17

which in turn might lead to reduced delay and faster emergency teams response times.

### 5.1. Traffic control scheme

The heuristic traffic control logic used in this research is an extension of the algorithm proposed by [29]. The main control algorithms' principle is to select signal stages and adjust their green durations in real-time based on a weighted signal stages score, which is reflecting vehicles' distance to the stop line on the lanes associated with the stages. The weights used in this score are higher for vehicles that report shorter distances from the intersection in an attempt to prioritize them and increase the total throughput.

For this research, this traffic control algorithm was augmented with the Emergency Vehicle preemption scheme. The prioritization mechanism is an override module incorporated into the described traffic control algorithm. When an incoming EV is detected, its ETA is estimated based on reported location and speed data. Each second, the control logic evaluates (and reevaluates) two possible actions:

- If EV signal group current status is red, the algorithm estimates the last possible switching point to green so that EV delay is avoided or minimized. The latest possible switching point allows us to provide as much green as possible to conflicting movements and reduces the possible delay from the EV prioritization actions.
- If the EV status is green, the algorithm evaluates two possible actions, holding the green for the EV direction, or, if ETA is long enough, terminating green in order to provide green to the conflicting movements before switching back to the EV direction (aka recall).

In order to make more efficient and precise decisions, using CV telematics data, the algorithm calculates and estimates queue lengths at the expected EV arrival moment. Queue clearance times are then calculated and incorporated into the decision process regarding green switching points timing. Queue estimation is based on CV transmitted location, speed and destination. In consequence, the precision of the calculations and the resulting decisions are highly dependent on the V2I data communication quality.

The proposed control scheme demonstrates a possible utilization of the MLR estimator. If the current message loss rate is high, it is reasonable to suspect possible inaccuracies in EV preemption actions. Specifically, imperfect communication leads to queue length underestimation because of the lower number of vehicles being able to communicate their data. The underestimation of queue length consequently leads to a miscalculation of estimated green switching points leading to an increased EV delay.

In the case of high MLR values, to compensate for possible higher than estimated queue clearance times, ETA value and EV green switch point are adjusted to an earlier point in time. By doing so the algorithm is forced to make an earlier switch to EV Signal Group green, providing a safety margin to minimize possible delay due to communications quality related miscalculations. An earlier switching point will compensate for a possible underestimation of the queue ahead of the EV vehicle,

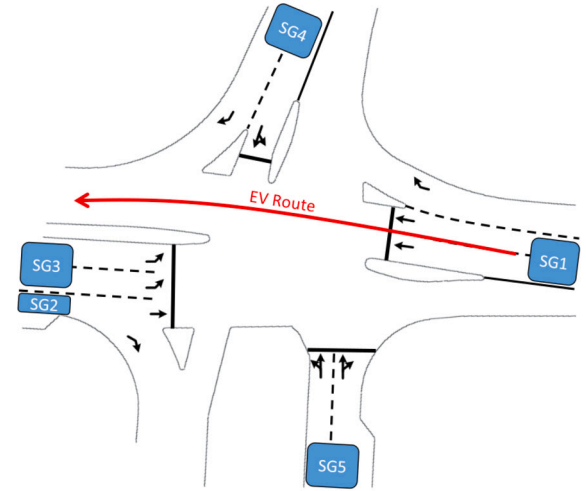


Fig. 7. Showcase intersection layout.

which needs to be cleared and might eliminate a costly, misplaced control action, such as an unjustified recall.

Once the EV crosses the stop line, the adaptive nature of the base algorithm helps to minimize the disturbance caused by the preemptive action. Holding the green or making an earlier switch leads to longer queues for conflicting signal groups, which in turn leads to larger stage scores and higher priority and longer green duration for these stages in the next signal cycle. This principle ensures the compensation of the signal groups for the lost green in the previous cycle and minimizes the delay caused by the EV preemption actions.

To showcase the usage of the proposed MLR metric in EV preemption algorithm and to demonstrate the potential benefits of its utilization, we use the same intersection model as in Section 4.1 (Hanita-Trumpeldor streets in the city of Haifa) but with an augmented EV preemption signal control algorithm. This specific intersection was chosen as a representative site for EV preemption showcase due to the intersection's relative proximity to the ambulance depot and the availability of traffic counts. The layout of the intersection is presented in Fig. 7. In reality, EV vehicles typically arrive from the east, utilizing Signal Group 1. The vehicle volumes scenario presented in Table 7 is based on the morning rush hour traffic counts. It should be noted here that, following the results demonstrated in the previous section, as the volumes of SG1 are high, the MLR accuracy is high as well.

### 5.2. Communication model aspects for EV preemption experiments

The approaching emergency vehicle sends its telemetry data to the Intersection Controller upon its arrival in the simulated area. In practice, the communication link between the emergency vehicle and IC is likely to be established using C-V2X, or any other standard or proprietary technology using a licensed spectrum. Hence, we assumed the link to be unaffected by the severe communication conditions present in the DSRC channel and therefore be essentially lossless.

**Table 7**

Morning rush hour demand scenario - Signal Group volumes and Signal-to-Noise Penalty settings for the case study simulations.

Signal Group / Direction	Volume [veh/hr]	SNR Penalty [dB]
SG1 - East	1073	20
SG2 - West	315	0
SG3 - West	713	
SG4 - North	534	0
SG5 - South	61	0

The data necessary to estimate the value of MLR are collected using DSRC-based V2I communication. As the DSRC was found to be the most challenging communication technology in terms of the MLR variation, see Section 4.2 for more details, we have decided to run the case study just for this communication technology as it allows to showcase nicely capabilities of the proposed MLR estimator. Moreover, it is worth noting here that the C-V2X was presumed to be deployed as one of the communication alternatives when it comes to the communication link between the emergency vehicle and IC in this work. The settings of the SNR Penalty used for the showcase are presented in Table 7. All the intersection approaches experienced significant communication disruptions. Moreover, the communication in the East approach, which the EV uses to approach the intersection, is subject to severe interference. The remaining simulation parameters related to the communication network are the same as defined in Section 4.1.

### 5.3. Showcase methodology

MLR estimator usage showcase is based on 50 pairs of simulation runs - each pair has the same simulation seed, ensuring identical traffic conditions at the moment of EV initial detection. In each pair two operational scenarios are considered:

- A baseline scenario, where no ETA adjustments are made. In this case, a higher delay to EV may occur due to a downstream queue underestimation or unjustified recall action because of CVs inability to report its location data.
- An alternative scenario, where the MLR estimator is utilized to adjust EV ETA to compensate for possible communication faults related to inaccuracies in control decisions. Lower delay to EV is expected as a bigger safety margin exists in control decisions and longer green durations are provided to clear the downstream queue.

It should be mentioned that there are cases where, in both scenarios, for the same seed, identical EV preemption control decisions will be made by the algorithm. Such cases are:

- At EV initial detection the measured MLR is low. In this case, there's no need to adjust EV ETA and the control decision will be the same as in the baseline scenario.
- EV SG is currently green or is switching to green and by algorithm estimation there's not enough time to perform a recall action. In this case, in both scenarios, the algorithm has no choice but to hold the green light until EV passage.

The occurrence of the described phenomena depends entirely on the existing traffic conditions and SG states at the moment of EVs initial detection. As there are no adjacent signalized intersections upstream at the East approach, EV arrival time at the detection zone is randomized for over 50 experiments.

Each simulation run is 20 minutes long with 10 minutes warm-up period, 5 minutes EV random arrival window, and 5 additional minutes to measure the performance in a recovery period after the preemption action.

**Table 8**

An increase in average delay for CV traffic in MLR-based preemption control scheme.

Signal Group	Volume [veh/hr]	Number of lanes	Average Delay increase [seconds]
SG1	1073	2	0.5
SG2	315	1	0.1
SG3	713	2	0.8
SG4	534	1	11.6
SG5	61	2	5.1

### 5.4. Results

The simulation results demonstrate the benefits and costs of the MLR estimator integration into EV preemption signal control algorithm. A paired t-test for 50 simulation result pairs shows that a statistically significant (p-value < 0.0001) decrease in EV delay (Fig. 8a) is achieved by utilizing MLR estimator data in signal control logic. The reduction of EV delay comes at a cost - a slight increase in average delay for other vehicles (see Fig. 8b) due to earlier switching points to EV green.

It should be mentioned however that some SGs experience higher, while still reasonable, delays than others, as shown in Table 8. This imbalance in the increased delay is related to the operating principle of the base CV control algorithm - throughput maximization. As described in Section 5.1, in the cycle after the preemptive action the Signal Stage order and durations are adjusted based on the signal stages scores. The highest score stages are served first and get longer durations of green. Based on the throughput maximization principle of the algorithm, the highest score is allocated to SGs with more lanes and higher volumes with the number of lanes being a more dominant factor. As a result, a single lane SG4 experiences the highest increase in an average delay of 11.6 seconds, and a low volume SG5 the second highest (i.e., 5.1 seconds). SG2 is an exception in this case as it benefits from the green duration of high volume and two-lane SG3 located at the same approach and in the same Signal Stage.

## 6. Discussion and conclusions

In this paper, an analytical approach to estimate the performance of vehicular communication in terms of MLR has been developed. The approach utilizes existing message transmissions in a vehicular network to estimate the intensity of the arrival flow of vehicles into the intersection. Therefore, it eliminates the need for additional data transfers in bandwidth-limited vehicular networks. Based on the estimated traffic intensity, the number of messages sent by approaching vehicles, and subsequently the MLR, are estimated.

The performance of the presented MLR estimation approach in terms of MAE and Spearman's rank correlation coefficient was assessed by the federated telco-traffic simulation experiments. The simulation results indicate that the presented approach is applicable in a wide range of communication environments. Apart from the highest investigated SNR Penalty value of 30 dB, when communication was barely possible (MLR is around 80%). The performance of the presented estimation approach remained stable for the remaining values of the SNR Penalty (i.e., 0, 20, and 25 dB).

The simulation results further suggest that the MLR estimation approach presented herein achieves optimum performance when the volume of vehicles approaching the intersection is at least 400 vehicles per hour. Hence, the benefits of applying the proposed MLR estimation approach can be best reaped at moderately and highly busy intersections. Similarly, the intersection leg length affects the performance, although the effect is not as pronounced as in the case of the vehicle volume. A slightly improved performance was observed for 200 m intersection leg length compared to 100 m leg length.

Furthermore, we demonstrated the applicability of the developed estimation approach in a showcase concerning intersection preemption

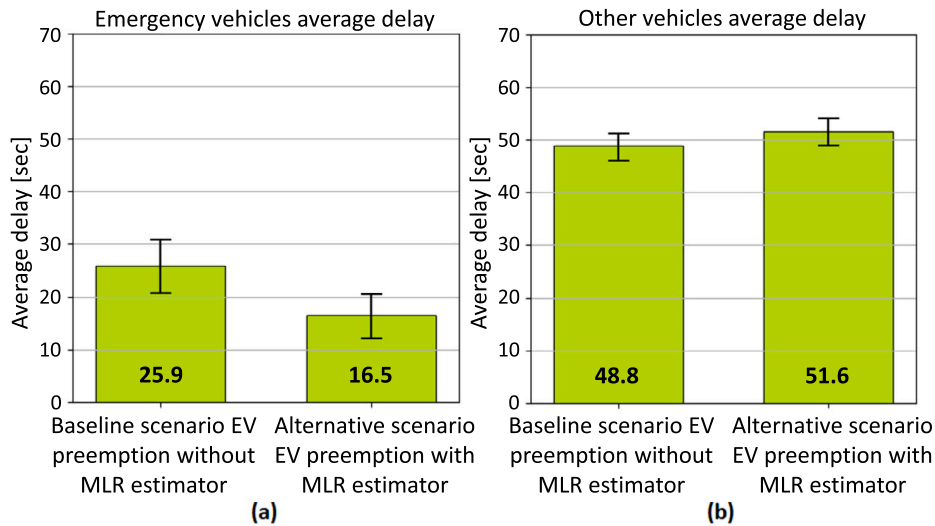


Fig. 8. Average delay and 95% confidence intervals: (a) Emergency vehicles average delay. (b) Other vehicles average delay.

for an approaching emergency vehicle. The simulation results indicate that the MLR estimator provides a safety margin for preemption actions during poor communications conditions and is beneficial for emergency vehicles.

Modern traffic signal controllers are capable of storing and executing sophisticated traffic signal logic and exchanging data with other devices (such as road-side units and on-board units). Therefore, existing control devices are capable of implementing the proposed methodology. Kavitha et al. in [61] present one possible hardware architecture that demonstrates such capabilities.

The benefits of MLR estimation were demonstrated in this work for a single intersection. When coordinated intersections are considered, especially when the distance between intersections is small, the benefits are expected to be influenced by the constraints imposed by the coordination requirements. More specifically, the decrease in flexibility concerning the phase composition may somewhat diminish the MLR estimation advantages, though not to the extent of erasing them entirely [29]. Further research regarding such network configuration is called for.

In our future work, we also aim to address mechanisms to either detect or estimate the number of hidden vehicles based on advanced methods of data analysis and machine learning. Furthermore, we would like to validate the obtained simulation results by deploying the MLR estimator at a real intersection.

#### Declaration of competing interest

The authors declare that they have no known competing financial interests or personal relationships that could have appeared to influence the work reported in this paper.

#### Data availability

We have shared the link to the repository containing MLR estimator implementation and the simulation files for the OMNeT++ in the References section of the paper.

#### Acknowledgements

This work was supported in part by grant 3-15353 from the Ministry of Science and Technology, Israel and in part by the Slovak Research and Development Agency under Contract SK-IL-RD-18-005.

The work of Ľuboš Buzna was supported in part by the Scientific Grant Agency of the Ministry of Education, Science, Research and Sport

of the Slovak Republic under the project VEGA 1/0077/22 “Innovative prediction methods for optimization of public service systems” and project VEGA 1/0216/21 “Design of emergency systems with conflicting criteria with the tools of artificial intelligence”, in part by the Slovak Research and Development Agency under the project APVV-19-0441 “Allocation of limited resources to public service systems with conflicting quality criteria”, and in part by the Operational Program Integrated Infrastructure 2014–2020 “Innovative Solutions for Propulsion, Power, and Safety Components of Transport Vehicles” through the European Regional Development Fund under grant ITMS313011V334.

The authors would like to thank Dr. Marek Drličiak and Prof. Ján Čelko for their invaluable support in facilitating the use of simulation tools essential for this research and Prof. Tatiana Kováčiková and Prof. Milan Dado for useful discussions and comments.

#### Appendix A. Extended list of simulation parameters

Table A.9

List of the most important simulation parameters of the DSRC and their values.

Parameter	Value
MAC Type	According to IEEE 802.11-2016 with parameter <i>dot11OCBAActivated</i> set to true
Queue capacity	100 frames
Radio operation mode	802.11p
Modulation	QPSK
Coding rate	1/2
Transfer rate	6 Mbit/s
LLC operation mode	According to IEEE/ISO/IEC 8802-2-1998 Type 1 – unacknowledged connectionless mode
Channel bandwidth	10 MHz
Carrier frequency	5,900 MHz
Radio receiver SNIR threshold	4 dB
Radio receiver min. sensitivity	-85 dBm
Radio transmitter power	20 mW
Antenna type	Isotropic Antenna
Car antenna height	1.895 m
RSU antenna height	5.897 m
EDCA access category	AC_VO
Used EDCA AC AIFSN	2
EDCA AC CWmin	3
EDCA AC CWmax	7
Max MAC MTU	1500 B
Pathloss model	Two Ray Interference model
Message length	300 B
Message generation frequency	1 Hz

Table A.10

List of the most important simulation parameters of the 4G-based and 5G-based C-V2X and their values.

Parameter	Value in 5G-based C-V2X	Value in 4G-based C-V2X
Operation mode	Vehicle-to-Network in infrastructural mode (Uu)	Vehicle-to-Network in infrastructural mode (Uu)
Scenario	Urban Macrocell	Urban Macrocell
Pathloss model	3D-Uma Path Loss Model as defined in 3GPP TR 36.873 (Table 7.2-1)	3D-Uma Path Loss Model as defined in 3GPP TR 36.873 (Table 7.2-1)
Number of carriers	1	1
Number of subcarriers per RB	12	12
Modulation	QPSK, 16 QAM, 64 QAM, 256 QAM	QPSK, 16 QAM, 64 QAM
Summary feedback confidence function lower bound	5 ms	5 ms
Summary feedback confidence function upper bound	20 ms	20 ms
Feedback historical base capacity in DL	5	5
Feedback historical base capacity in UL	5	5
Target BLER	0.01	0.01
BLER Shift	5	5
Carrier frequency	2,400 MHz	2,400 MHz
Number of resource blocks	100	100
Numerology index	2	not applicable – 15 kHz subcarrier spacing
gNB/eNB height	25 m	25 m
Car antenna height	1.895 m	1.895 m
Building height	20 m	20 m
Street width	20 m	20 m
Correlation distance	50	50
Channel matrix eigenvalues thresholds	LambdaMinTh = 0.02, LambdaMaxTh = 0.2, LambdaRatioTh = 20	LambdaMinTh = 0.02, LambdaMaxTh = 0.2, LambdaRatioTh = 20
Proportional Fair Alpha	0.95	0.95
Conflict Graph Threshold	-90 dBm	-90 dBm
RSRQ shift	22	22
RSRQ scale	1	1
HARQ reduction	0.2	0.2
Car Tx direction	omnidirectional	omnidirectional
Car Tx angle	0	0
Antenna gain car	0	0
Antenna gain gNB/eNB	18 dBi	18 dBi
Tx power car	26 dBm	26 dBm
Tx power gNB/eNB	46 dBm	46 dBm
Thermal noise	-104.5 dBm	-104.5 dBm
Car noise figure	7 dB	7 dB
gNB/eNB noise figure	5 dB	5 dB
Cable loss	2 dB	2 dB
Fading type	Jakes	Jakes
Fading paths	6	6
RMS Delay Spread	363 ns	363 ns
Min. RSSI	-99 dBm	-99 dBm
Path loss coefficient	2	2
Resource allocation type	Localized	Localized
HARQ processes	8	8
Max. HARQ RTX	3	3
Scheduling discipline	MAXCI	MAXCI
Grant type (UL and DL)	FITALL	FITALL
Grant size (UL and DL)	4 GB	4 GB
gNB/eNB network interface card delay	0 s	0 s
PDCCP to RRC header compression	disabled	disabled
MAC queue size	2 MB	2 MB
Network layer protocol	IPv4	IPv4
Transport layer protocol	UDP	UDP
Message length	300 B	300 B
Message generation frequency	1 Hz	1 Hz

## References

- [1] E. Uhlemann, Introducing connected vehicles [connected vehicles], *IEEE Veh. Technol. Mag.* 10 (1) (2015) 23–31, <https://doi.org/10.1109/MVT.2015.2390920>.
- [2] R.K. Schmidt, B. Kloiber, F. Schüttler, T. Strang, Degradation of communication range in VANETs caused by interference 2.0 - real-world experiment, in: T. Strang, A. Festag, A. Vinel, R. Mehmood, C. Rico Garcia, M. Röckl (Eds.), *Communication Technologies for Vehicles*, Springer Berlin Heidelberg, Berlin, Heidelberg, 2011, pp. 176–188.
- [3] S.E. Carpenter, Obstacle shadowing influences in VANET safety, in: 2014 IEEE 22nd International Conference on Network Protocols, 2014, pp. 480–482.
- [4] R.B. Vukmir, Survival from prehospital cardiac arrest is critically dependent upon response time, *Resuscitation* 69 (2) (2006) 229–234, <https://doi.org/10.1016/j.resuscitation.2005.08.014>, <https://www.sciencedirect.com/science/article/pii/S0300957205003680>.
- [5] N. Challands, The relationships between fire service response time and fire outcomes, *Fire Technol.* 46 (3) (2010) 665–676, <https://doi.org/10.1007/s10694-009-0111-y>.
- [6] C.-L. Lee, C.-Y. Huang, T.-C. Hsiao, C.-Y. Wu, Y.-C. Chen, I.-C. Wang, Impact of vehicular networks on emergency medical services in urban areas, *Int. J. Environ. Res. Public Health* 11 (11) (2014) 11348–11370, <https://doi.org/10.3390/ijerph11111348>.
- [7] S. Lee, A. Lim, An empirical study on ad hoc performance of DSRC and Wi-Fi vehicular communications, *Int. J. Distrib. Sens. Netw.* 9 (11) (2013) 482695, <https://doi.org/10.1155/2013/482695>.
- [8] F. Bai, H. Krishnan, Reliability analysis of DSRC wireless communication for vehicle safety applications, in: 2006 IEEE Intelligent Transportation Systems Conference, 2006, pp. 355–362.
- [9] Y. Wang, J. Hu, Y. Zhang, C. Xu, Reliability evaluation of IEEE 802.11p-based vehicle-to-vehicle communication in an urban expressway, *Tsinghua Sci. Technol.* 20 (4) (2015) 417–428, <https://doi.org/10.1109/TST.2015.7173456>.
- [10] E.E. González, D. Garcia-Roger, J.F. Monserrat, LTE/NR V2X communication modes and future requirements of intelligent transportation systems based on MR-DC architectures, *Sustainability* 14 (7) (2022) 3879.
- [11] C. Ghodhbane, M. Kassab, S. Maaloul, H. Aniss, M. Berbineau, A study of LTE-V2X mode 4 performances in a multiapplication context, *IEEE Access* 10 (2022) 63579–63591.
- [12] L. Zhao, J. Fang, J. Hu, Y. Li, L. Lin, Y. Shi, C. Li, The performance comparison of LTE-V2X and IEEE 802.11 p, in: 2018 IEEE 87th Vehicular Technology Conference (VTC Spring), IEEE, 2018, pp. 1–5.
- [13] T. Bey, G. Towolde, Evaluation of DSRC and LTE for V2X, in: 2019 IEEE 9th Annual Computing and Communication Workshop and Conference (CCWC), IEEE, 2019, pp. 1032–1035.
- [14] M. Karoui, A. Freitas, G. Chalhoub, Performance comparison between LTE-V2X and ITS-G5 under realistic urban scenarios, in: 2020 IEEE 91st Vehicular Technology Conference (VTC2020-Spring), IEEE, 2020, pp. 1–7.
- [15] T.V. Nguyen, P. Shailesh, B. Sudhir, G. Kapil, L. Jiang, Z. Wu, D. Malladi, J. Li, A comparison of cellular vehicle-to-everything and dedicated short range communication, in: 2017 IEEE Vehicular Networking Conference (VNC), IEEE, 2017, pp. 101–108.
- [16] Z.H. Mir, F. Filali, On the performance comparison between IEEE 802.11 p and LTE-based vehicular networks, in: 2014 IEEE 79th Vehicular Technology Conference (VTC Spring), IEEE, 2014, pp. 1–5.
- [17] M. Wang, M. Winbjork, Z. Zhang, R. Blasco, H. Do, S. Sorrentino, M. Belleschi, Y. Zang, Comparison of LTE and DSRC-based connectivity for intelligent transportation systems, in: 2017 IEEE 85th Vehicular Technology Conference (VTC Spring), IEEE, 2017, pp. 1–5.
- [18] P. Roux, S. Sesia, V. Mannoni, E. Perraud, System level analysis for ITS-G5 and LTE-V2X performance comparison, in: 2019 IEEE 16th International Conference on Mobile Ad Hoc and Sensor Systems (MASS), IEEE, 2019, pp. 1–9.
- [19] T. Petrov, L. Sevcik, P. Počta, M. Dado, A performance benchmark for dedicated short-range communications and LTE-based cellular-V2X in the context of vehicle-to-infrastructure communication and urban scenarios, *Sensors* 21 (15) (2021) 5095.
- [20] G. Cecchini, A. Bazzi, B.M. Masini, A. Zanella, Performance comparison between IEEE 802.11 p and LTE-V2V in-coverage and out-of-coverage for cooperative awareness, in: 2017 IEEE Vehicular Networking Conference (VNC), IEEE, 2017, pp. 109–114.
- [21] V. Mannoni, V. Berg, S. Sesia, E. Perraud, A comparison of the V2X communication systems: ITS-G5 and C-V2X, in: 2019 IEEE 89th Vehicular Technology Conference (VTC2019-Spring), IEEE, 2019, pp. 1–5.
- [22] V. Maglogiannis, D. Naudts, S. Hadiwardoyo, D. van den Akker, J. Marquez-Barja, I. Moerman, Experimental V2X evaluation for C-V2X and ITS-G5 technologies in a real-life highway environment, *IEEE Trans. Netw. Serv. Manag.* (2021).
- [23] J. Zhao, X. Gai, X. Luo, Performance comparison of vehicle networking based on DSRC and LTE technology, in: *International Conference on Intelligent Transportation Engineering*, Springer, 2022, pp. 722–738.
- [24] R. Molina-Masegosa, J. Gosalvez, M. Sepulcre, Comparison of IEEE 802.11 p and LTE-V2X: an evaluation with periodic and aperiodic messages of constant and variable size, *IEEE Access* 8 (2020) 121526–121548.

- [25] T. Petrov, P. Počta, T. Kovacicova, Benchmarking 4G and 5G-based cellular-V2X for vehicle-to-infrastructure communication and urban scenarios in cooperative intelligent transportation systems, *Appl. Sci.* 12 (19) (2022) 9677.
- [26] R. Liu, Y. Ren, H. Yu, Z. Li, H. Jiang, Connected and automated vehicle platoon maintenance under communication failures, *Veh. Commun.* 35 (2022) 100467, <https://doi.org/10.1016/j.vehcom.2022.100467>, <https://www.sciencedirect.com/science/article/pii/S2214209622000146>.
- [27] H. Jiang, S. Chen, Y. Yang, Z. Jie, H. Leung, J. Xu, L. Wang, Estimation of packet loss rate at wireless link of VANET-RPLE, in: 2010 6th International Conference on Wireless Communications Networking and Mobile Computing (WiCOM), 2010, pp. 1–5.
- [28] O. Alzamaz, I. Mahgoub, An enhanced directional greedy forwarding for VANETs using link quality estimation, in: 2016 IEEE Wireless Communications and Networking Conference, 2016, pp. 1–7.
- [29] I. Finkelberg, T. Petrov, A. Gal-Tzur, N. Zarkhin, P. Počta, T. Kováčiková, L. Buzna, M. Dado, T. Toledo, The effects of vehicle-to-infrastructure communication reliability on performance of signalized intersection traffic control, *IEEE Trans. Intell. Transp. Syst.* 23 (9) (2022) 15450–15461, <https://doi.org/10.1109/ITTS.2022.3140767>.
- [30] C. Campolo, A. Molinaro, A. Vinel, Understanding the performance of short-lived control broadcast packets in 802.11p/wave vehicular networks, in: 2011 IEEE Vehicular Networking Conference (VNC), 2011, pp. 102–108.
- [31] J.P. Pell, J.M. Sirel, A.K. Marsden, I. Ford, S.M. Cobbe, Effect of reducing ambulance response times on deaths from out of hospital cardiac arrest: cohort study, *BMJ* 322 (7299) (2001) 1385–1388, <https://doi.org/10.1136/bmj.322.7299.1385>, <https://www.bmj.com/content/322/7299/1385>.
- [32] H. Su, K. Shi, L. Jin, J.Y.J. Chow, V2I connectivity-based dynamic queue-jump lane for emergency vehicles: a deep reinforcement learning approach, arXiv:2008.00335, 2021.
- [33] H. Xie, S. Karunasekera, L. Kulik, E. Tanin, R. Zhang, K. Ramamohanarao, A simulation study of emergency vehicle prioritization in intelligent transportation systems, in: 2017 IEEE 85th Vehicular Technology Conference, VTC Spring, 2017, pp. 1–5.
- [34] H. Noori, L. Fu, S. Shiravi, Connected-vehicle-based traffic signal control strategy for emergency vehicle preemption, in: TRB 95th Annual Meeting Compendium of Papers, 2006, pp. 16–6763.
- [35] X. Qin, A.M. Khan, Control strategies of traffic signal timing transition for emergency vehicle preemption, *Transp. Res., Part C, Emerg. Technol.* 25 (2012) 1–17, <https://doi.org/10.1016/j.trc.2012.04.004>, <https://www.sciencedirect.com/science/article/pii/S0968090X1200054X>.
- [36] V. Paruchuri, Adaptive preemption of traffic for emergency vehicles, in: 2017 UKSim-AMSS 19th International Conference on Computer Modelling & Simulation (UKSim), 2017, pp. 45–49.
- [37] S. Humagain, R. Sinha, E. Lai, P. Ranjitkar, A systematic review of route optimisation and pre-emption methods for emergency vehicles, *Transp. Rev.* 40 (1) (2020) 35–53, <https://doi.org/10.1080/01441647.2019.1649319>.
- [38] W. Yu, W. Bai, W. Luan, L. Qi, State-of-the-art review on traffic control strategies for emergency vehicles, *IEEE Access* 10 (2022) 109729–109742, <https://doi.org/10.1109/ACCESS.2022.3213798>.
- [39] M. Cao, V.O. Li, Q. Shuai, A gain with no pain: exploring intelligent traffic signal control for emergency vehicles, *IEEE Trans. Intell. Transp. Syst.* 23 (10) (2022) 17899–17909.
- [40] D. Das, N.V. Altekhar, K.L. Head, F. Saleem, Traffic signal priority control strategy for connected emergency vehicles with dilemma zone protection for freight vehicles, *Transp. Res. Rec.* 2676 (1) (2022) 499–517.
- [41] G. James, D. Witten, T. Hastie, R. Tibshirani, *An Introduction to Statistical Learning: with Applications in R*, Springer, 2013.
- [42] ETSI, ETSI EN 302 637: intelligent transport systems (ITS); vehicular communications; basic set of applications; part 2: specification of cooperative awareness basic service, [https://www.etsi.org/deliver/etsi\\_en/302600\\_302699/30263702/01.03.01\\_30/en\\_30263702v010301v.pdf](https://www.etsi.org/deliver/etsi_en/302600_302699/30263702/01.03.01_30/en_30263702v010301v.pdf). (Accessed 8 February 2023), 2012.
- [43] MLR estimator implementation and simulation files, <https://github.com/petrovtsk/MLR-Estimator>. (Accessed 25 October 2023), 2023.
- [44] T. Petrov, I. Finkelberg, N. Zarkhin, P. Počta, L. Buzna, A. Gal-Tzur, T. Kovacicova, T. Toledo, M. Dado, A framework coupling VISSIM and OMNeT++ to simulate future intelligent transportation systems, *Commun. Sci. Lett. Univ. Zilina* 23 (2) (2021) C23–C29, <https://komunikacie.uniza.sk/artkey/csl-202102-0011.php>.
- [45] C. Sommer, Z. Yao, R. German, F. Dressler, Simulating the influence of IVC on road traffic using bidirectionally coupled simulators, in: *IEEE INFOCOM Workshops 2008*, 2008, pp. 1–6.
- [46] C. Sommer, R. German, F. Dressler, Bidirectionally coupled network and road traffic simulation for improved IVC analysis, *IEEE Trans. Mob. Comput.* 10 (1) (2011) 3–15, <https://doi.org/10.1109/TMC.2010.133>.
- [47] S.Y. Wang, C.L. Chou, Y.H. Chiu, Y.S. Tzeng, M.S. Hsu, Y.W. Cheng, W.L. Liu, T.W. Ho, NCTUns 4.0: an integrated simulation platform for vehicular traffic, communication, and network researches, in: 2007 IEEE 66th Vehicular Technology Conference, 2007, pp. 2081–2085.
- [48] OMNeT++, OMNeT++ discrete event simulator, <https://omnetpp.org>. (Accessed 8 February 2023), 2023.
- [49] P. Alvarez Lopez, M. Behrisch, L. Bieker-Walz, J. Erdmann, Y.-P. Flötteröd, R. Hilbrich, L. Lücken, J. Rummel, P. Wagner, E. Wießner, Microscopic traffic simulation using SUMO, in: 2019 IEEE Intelligent Transportation Systems Conference (ITSC), IEEE, 2018, pp. 2575–2582, <https://elib.dlr.de/127994/>.
- [50] G. Nardini, D. Sabella, G. Stea, P. Thakkar, A. Virdis, Simu5G—an OMNeT++ library for end-to-end performance evaluation of 5G networks, *IEEE Access* 8 (2020) 181176–181191, <https://doi.org/10.1109/ACCESS.2020.3028550>.
- [51] INET, INET framework: an open-source OMNeT++ model suite for wired, wireless and mobile networks, <https://inet.omnetpp.org>, 2023. (Accessed 8 February 2023).
- [52] IEEE, IEEE standard for information technology—telecommunications and information exchange between systems local and metropolitan area networks—specific requirements - part 11: wireless LAN medium access control (MAC) and physical layer (PHY) specifications, <https://standards.ieee.org/ieee/802.11/5536/>. (Accessed 8 February 2023), 2016.
- [53] ETSI, ETSI TS 102 637-2: intelligent transport systems (ITS); vehicular communications; basic set of applications; part 2: specification of cooperative awareness basic service, [https://www.etsi.org/deliver/etsi\\_ts/102600\\_102699/10263702/01.02.01\\_60/ts\\_10263702v010201p.pdf](https://www.etsi.org/deliver/etsi_ts/102600_102699/10263702/01.02.01_60/ts_10263702v010201p.pdf). (Accessed 8 February 2023), 2011.
- [54] E.J. Jaselskis, J. Grigas, A. Brilingas, Dielectric properties of asphalt pavement, *J. Mater. Civ. Eng.* 15 (5) (2003) 427–434, [https://doi.org/10.1061/\(ASCE\)0899-1561\(2003\)15:5\(427\)](https://doi.org/10.1061/(ASCE)0899-1561(2003)15:5(427)), <https://ascelibrary.org/doi/abs/10.1061>.
- [55] V. Mannoni, V. Berg, S. Sesia, E. Perraud, A comparison of the V2X communication systems: ITS-G5 and C-V2X, in: 2019 IEEE 89th Vehicular Technology Conference (VTC2019-Spring), 2019, pp. 1–5.
- [56] ETSI, ETSI EN 302 663: intelligent transport systems (ITS); ITS-G5 access layer specification for intelligent transport systems operating in the 5 GHz frequency band, [https://www.etsi.org/deliver/etsi\\_en/302600\\_302699/302663/01.03.01\\_30/en\\_302663v010301v.pdf](https://www.etsi.org/deliver/etsi_en/302600_302699/302663/01.03.01_30/en_302663v010301v.pdf). (Accessed 8 February 2023), 2012.
- [57] 3rd generation partnership project TR 36.873: 3rd generation partnership project; technical specification group radio access network; study on 3D channel model for LTE (release 12), <https://portal.3gpp.org/desktopmodules/Specifications/SpecificationDetails.aspx?specificationId=2574>. (Accessed 30 July 2023), 2018.
- [58] C. Sommer, D. Eckhoff, A. Brummer, D.S. Buse, F. Hagenauer, S. Joerer, M. Segata, Veins – the open source vehicular network simulation framework, in: A. Virdis, M. Kirsche (Eds.), *Recent Advances in Network Simulation*, Springer, 2019.
- [59] 3rd generation partnership project TR 21.916: Technical specification group services and system architecture; release 16 description; summary of rel-16, <https://www.3gpp.org/specifications-technologies/releases/release-16>. (Accessed 30 July 2023), 2021.
- [60] ITU-R, Report ITU-R M.2292-0 - characteristics of terrestrial IMT-advanced systems for frequency sharing/interference analyses, ITU-R, Dec 2013.
- [61] Y. Kavitha, P. Satyanarayana, S.S. Mirza, Sensor based traffic signal pre-emption for emergency vehicles using efficient short-range communication network, *Measur. Sens.* 28 (2023) 100830, <https://doi.org/10.1016/j.measen.2023.100830>, <https://www.sciencedirect.com/science/article/pii/S2665917423001666>.